

COMBINATION OF LIDAR AND RADAR OBSERVATIONS TO RETRIEVE MICROPHYSICAL PROPERTIES OF BOUNDARY LAYER CLOUDS USING A NEW ANALYTICAL APPROACH

Damien Josset⁽¹⁾, Jacques Pelon⁽¹⁾, Alain Protat⁽²⁾, Martial Haeffelin⁽³⁾

⁽¹⁾ Service d'Aéronomie/IPSL, 4 place Jussieu B102 75252 Paris France, E-mail: damien.josset@aero.jussieu.fr

⁽²⁾ CETP/IPSL, 10-12 avenue de l'Europe 78140 Vélizy-Villacoublay France, E-mail: alain.protat@cetp.ipsl.fr

⁽³⁾ LMD/IPSL Ecole polytechnique, F91128 Palaiseau cedex France, E-mail : Martial.Haeffelin@lmd.polytechnique.fr

ABSTRACT

A case study analysis has been conducted on the diurnal cycle of boundary layer clouds observed at the IPSL station in Palaiseau (France) on the period from the 22nd to the 26th March 2004, during the CLOUDNET project. The cloud properties have been analysed using remote sensing (ground based radar and lidar), applying the Klett inversion method in a new way to retrieve microphysical properties of a stratocumulus cloud layer. Comparisons of results obtained on March 24th at the end of the morning with satellite observations (MODIS) and with forecasts from three numerical models (METEOFRANCE ARPEGE, UKMO Unified Model and ECMWF) are presented and discussed here.

1. INTRODUCTION

To retrieve warm cloud microphysical properties from combined lidar and radar data analysis as previously proposed using an analytical approach [1], we need to derive the value of extinction in an accurate way. This is made difficult for water clouds as the signal is rapidly attenuated, and non-linearities may occur.

In this paper, we propose to use the inherent instable behavior of the Klett prograde inversion [2] as a way to retrieve an effective extinction to backscatter lidar ratio (S'). The word "effective" stress the advantage of this method that can be used when the lidar is not well calibrated or when multiple scattering occurs. The cloud top retrieved by the radar data adds another constraint that lowers the error made on S' . The lidar effective extinction (second order momentum of the droplet size distribution –DSD–) and radar reflectivity (sixth order momentum of the DSD) are then used to derive the cloud microphysics assuming a gamma shaped DSD. In section 2, we present the theoretical background of the method. In section 3, we will expose the method itself and give results from simulations for illustration purpose. In section 4, we will test it on a case study and use it to retrieve the microphysical properties of a sample of stratocumulus cloud and we will finish with a few conclusive words in section 5.

2. THEORY

The hypothesis of a constant extinction to backscatter lidar ratio S is well realized for the range of droplet size commonly observed in stratocumulus [3], [4], [5]. Under this assumption, and including multiple scattering as a coefficient η in the optical depth, as proposed by Platt [6], so that the lidar ratio S becomes $S'=\eta S$, hereafter called effective lidar ratio, and extinction α becomes the effective extinction $\alpha'=\eta\alpha$, a simple form of the unstable Klett's analytical inversion solution for lidar returns can be written as

$$\alpha'(R) = \frac{S' P}{1 - 2 \int_0^R S' P dr} \quad (1)$$

Where P is the signal returned from the lidar in physical units (i.e. the attenuated backscatter coefficient). R is the range between the atmospheric sample and the telescope. The integral term could become greater than 1 if a wrong value of $S'P$ is used during the retrieval and lead to negative value of the extinction. Assuming a correctly normalized value of P and writing $\delta S'$ the error made on S' , the total error on the restituted effective extinction $\delta\alpha'$ can be written

$$\frac{\delta\alpha'}{\alpha'} = \frac{\frac{\delta S'}{S'}}{e^{-2\tau} + \frac{\delta S'}{S'}(e^{-2\tau} - 1)} \quad (2)$$

For the rest of this study, we will use the term unstable when negative value occur ($\delta\alpha' < -\alpha'$).

The instability threshold is then defined by

$$e^{-2\tau} = \frac{\delta S'}{S' + \delta S'} \quad (3)$$

Equation (3) means that the higher the value of the optical depth, the smaller will be the uncertainty $\delta S'$, and using this condition at the cloud top height determined by the radar data will give better results.

3. SIMULATION

Assuming a constant value of S and a linear variation of the extinction α with height inside a cloud, the attenuated backscatter coefficient can be calculated. We can then use equation (1) using different values of S' . The last value of S' giving non negative extinction at cloud top will be used for the restitutions. As an example a simulated cloud with a geometrical depth of 400 m and an original value of S set equal to 20 has been considered.

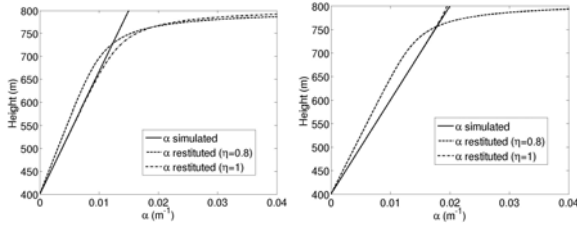


Fig. 1. Left: simulated extinction α (solid line) for $\tau=3$, the restituted extinction without multiple scattering (dashed line) $\eta=1$, $S'=20.04$ and with multiple scattering (dashed dotted line) $\eta=0.8$, $S'=16.13$. Right : same picture for $\tau=4$, as expected the accuracy is better for $\eta=1$ than for multiple scattering where $S'=16.02$ for $\eta=0.8$.

We performed the simulation with varying optical thickness. Results are reported in Fig. 1. for $\tau=3$, $\tau=4$ and S' varying from 0 to 80 by step of 0.01. As stated by equation (3), the accuracy of the restitution is better for higher optical thickness and without multiple scattering. Indeed, the difference is hardly visible between the original value of α and its restitution for $\tau=4$ and $\eta=1$. For the other cases (Fig. 1), the restitution is in good agreement with the expected value in the lower part of the cloud and become unrealistically high near the top of the cloud.

Equation (2) can be rewritten for a linear variation of the extinction with the constant slope K to find the height above cloud base z for a given relative error on α' and S' ($\frac{\delta \alpha'}{\alpha'} > \frac{\delta S'}{S'}$ for stable solution).

$$z = \sqrt{\frac{1}{K} \ln \left(\frac{\frac{\delta \alpha'}{\alpha'} \left(1 + \frac{\delta S'}{S'} \right)}{\frac{\delta S'}{S'} \left(1 + \frac{\delta \alpha'}{\alpha'} \right)} \right)} \quad (4)$$

For $\tau=3$, $\frac{\delta \alpha'}{\alpha'} = 0.1$ and $\frac{\delta S'}{S'} = 0.002$, $z = 319$ m

4. APPLICATION TO A CASE STUDY

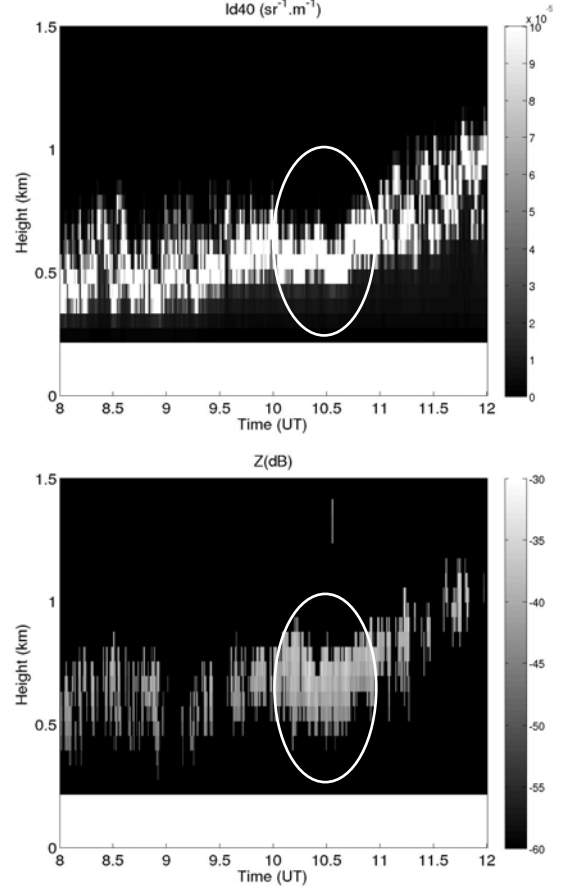


Fig. 2. Time evolution (quicklook) of the ceilometer signal (up) and radar signal (bottom) between 0800 UT and 1200 UT. The cloud pattern evolves from stratocumulus clouds in the morning to precipitating cumulus in the afternoon.

We have used observations made on 24th March 2004 at the IPSL observatory site in Palaiseau using a Vaisala LD40 ceilometer and the cloud radar RASTA developed by CETP/IPSL operating at 95 GHz [7]. This day was characterized by a stratocumulus cloudy layer in the morning and a more convective phase with cumulus in the afternoon (Fig. 2).

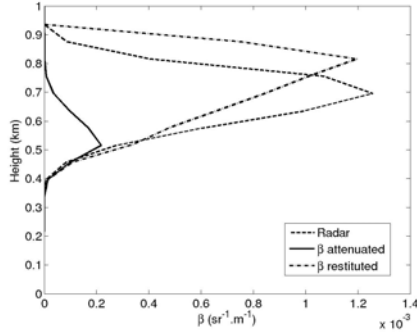


Fig.3. Radar (dashed line, arbitrary units) and ceilometer mean profile (10h-11h) the 24th march 2004 attenuated (solid line) and restituted by the method (dash dotted line).

Tab. 1. Mean radar signal (10h-11h), extinction restitution from the mean backscatter coefficient and microphysical properties retrieved by the radar/lidar algorithm

Height (km)	Z (10 ⁻⁷ mm ⁶ .m ⁻³)	α (10 ⁻⁴ m ⁻¹)	Nt (cm ⁻³)	LWC (10 ⁻⁶ kg.m ⁻³)	Re (μ m)
0.396	6.4	1.8	3	0.5	3.8
0.456	83	14	18	4.3	4.2
0.516	280	43	62	15	4.2
0.576	610	62	71	23	4.7
0.636	1000	86	66	29	5.2
0.696	1300	110	147	48	4.7
0.756	1100	130	125	41	4.7
0.816	410	160	404	45	3.3
0.876	87	98	219	15	2.8

The Tab. 1 restitutions correspond to a total optical thickness of 4.2.

We have calculated the microphysical properties of the cloud with the lidar and radar signal, assuming a normalized gamma size distribution for the water droplets, as given by

$$n(D) = N_w \frac{6}{3.67^4} \frac{(3.67 + \mu)^4}{\Gamma(\mu + 4)} \left(\frac{D}{D_0}\right)^\mu \exp\left(-\frac{(3.67 + \mu)D}{D_0}\right) \quad (5)$$

Where N_w is the normalized droplet concentration, D_0 is the median equivolumetric diameter and μ is the size parameter. Results are given in Tab. 1 (droplet concentration Nt , liquid water content LWC , effective radius Re for a size parameter $\mu=8$ (according to [5] $\mu+1$ mean value is 8.7 on continental clouds with a standard deviation of 6.3). For $\mu=2$, the changes with respect to

$\mu=8$ are +41% for Nt , -6% for Re and -25% for LWC . For $\mu=13$, they are -6% for Nt , +2% for Re and +9% for LWC . The difference between the effective value of S' (13.05) and the value calculated by a Mie code [9] ($S'=19.0$) can be attributed to both multiple scattering and lidar calibration error. The value of the multiple scattering factor obtained appears larger than the one obtained from the Eloranta code [8] for the values in Table 1. This may be due to ceilometer calibration error and will be further investigated.

We can compare the restituted optical thickness and effective radius at cloud top with the MODIS retrievals as TERRA was over France the same day at 11h20.

Fig. 4 shows the statistical distribution of the top cloud effective radius and optical thickness for 2500 MODIS pixels (corresponding to a 2500 km² area around the site).

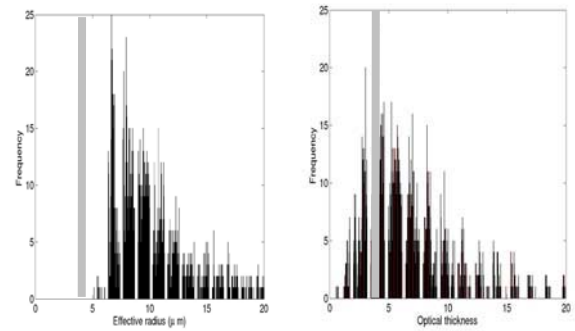


Fig. 4. Effective radius (left) and optical thickness (right) distribution as obtained by MODIS over an area of 50x50 km² near the observation site. The grey lines indicate the value restituted by the radar-lidar method.

Tab. 2. LWC restitution from the radar alone and lidar-radar

Height (km)	LWC (radar alone) (10 ⁻⁶ kg.m ⁻³)	LWC (lidar-radar) (10 ⁻⁶ kg.m ⁻³)
0,396	1	0.5
0,456	5.1	4.3
0,516	11	15
0,576	18	23
0,636	25	29
0,696	29	48
0,756	26	41
0,816	14	45
0,876	5.3	15

The restituted optical thickness seems in good agreement with the most occurring value retrieved by MODIS but the MODIS effective radii are much higher.

The LWC retrieved by this method and by a statistical

formula [9] using only the radar signal shows a good agreement (Tab. 2.)

Finally, Fig. 5. shows the comparisons of LWC and Re retrieved by this method with LWC and Re given by 3 numerical models.

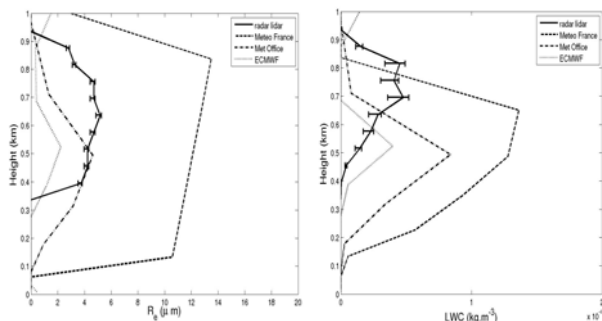


Fig. 5. (Left) Comparisons of the vertical distribution of the effective radius retrieved assuming $\mu = 8$ (solid line) –see text- with respect to model profiles : Meteo France ARPEGE (dashed line), UK Met Office (dash dotted line) and ECMWF (dotted line). (Right) Same but for the LWC . The error bars represent the impact of varying the DSD parameter μ from $\mu = 2$ to $\mu = 13$.

It shall be first noted that the geometrical thickness of the cloud is not well represented in the models, and they generally underestimate cloud top height and base. The maximum value of the effective radius is in close agreement for ECMWF, UKMO and retrievals. For ARPEGE Meteo France, the simulations were made using an old parameterization (Re depending only from the pressure) which gives much larger values. The LWC values are greater in the model simulations than retrieved mostly because of the altitude difference. The maximum retrieved LWC value is also close to the ones obtained with ECMWF or UKMO models having a prognostic scheme. Because of this offset in geometrical cloud thickness, the comparisons of liquid water path (LWP) make more sense. The radar lidar algorithm gives a value of 0.013 kg.m^{-2} , which is close to ECMWF value of 0.0093 kg.m^{-2} whereas the Unified model gives a larger results (0.024 kg.m^{-2}). ARPEGE gives about 4 times this (0.062 kg.m^{-2}). Assuming a constant effective radius value with height, equal to $6.7 \text{ }\mu\text{m}$ and an optical depth of 4, MODIS gives a value 0.018 kg.m^{-2} .

5. CONCLUSIONS

The approach developed in this paper gives a new procedure to retrieve the cloud extinction and further derive cloud microphysical properties. This method cannot be used accurately when optical depth is too small due to the unstable condition required using equation (3). This method allows to overcome a poor calibration of the lidar signal and multiple scattering

impact as a whole. Using the molecular backscattered signal from the clear atmosphere, the multiple scattering factor can be obtained. Results obtained are consistent with MODIS observations, and model simulations. Significant differences are however observed which may come from the boundary layer parameters used, leading to a smaller development of the BL. A more deeper research, studying more case will be further conducted to compare more cases.

6. ACKNOWLEDGEMENT

The data used in the study were provided by the CLOUDNET project and by the SIRTA team. The research reported in this paper was supported by Centre National d'Etudes Spatiales.

I would like to thank J. Tarniewicz for the software support.

REFERENCES

1. Pelon J., et al. *Optical and microphysical parameters of dense stratocumulus clouds during mission 206 of EUCREX'94 as retrieved from measurements made with the airborne lidar LEANDRE 1*, Atmospheric Research, Vol. 55, Issue 1, 47 – 64, 2000.
2. Klett J. D., *Stable analytical inversion solution for processing lidar returns*, Applied Optics, Vol. 20, N°2, 211 – 220, 1981.
3. Pinnick R. G., et al. *Backscatter and Extinction in Water Clouds*, Journal of Geophysical Research, Vol. 88, N°C11, 6787 – 6796, 1983.
4. O'Connor E. J., et al. *A Technique for Autocalibration of Cloud Lidar*, Journal of Atmospheric and oceanic technology, Vol. 21, 777 – 786, 2004.
5. Miles N. L., et al. *Cloud Droplet Size Distributions in Low-Level Stratiform Clouds*, Journal of Atmospheric science, Vol. 57, 295 – 311, 2000.
6. Platt C. M. R., *Lidar and Radiometric Observations of Cirrus Clouds*, Journal of The Atmospheric science, Vol. 30, 1191 – 1204, 1973.
7. Lhermitte R., *A 94-GHz Doppler Radar for Cloud Observations*, Journal of Atmospheric and Oceanic Technology, Vol. 4, 36 – 48, 1987.
8. Eloranta E. W., *Practical model for the calculation of multiply scattered lidar returns*, Applied Optics, Vol. 37, N°12, 2464 – 2472, 1998.
9. Bohren C., Huffman D., *Absorption and scattering of light by small particles*, New York Wiley, 1983.
10. Fox N. I., Illingworth A. J., *The Retrieval of Stratocumulus Cloud Properties by Ground-Based Cloud Radar*, Journal of Applied Meteorology, Vol. 36, 485 – 492, 1997.